Ultrasonic Characterization of Material Properties in Metal Components Additively Manufactured by Powder Bed Fusion

Kenneth Walton
Department of Chemical Engineering
University of Utah
Salt Lake City, UT
kenneth.walton@utah.edu

Mikhail Skliar
Department of Chemical Engineering
University of Utah
Salt Lake City, UT
mikhail.skliar@utah.edu

***Abstract*—We present the methodology for using pulsed-echo ultrasound to characterize the properties of additively manufactured (AM) metal components and their response to changes in the fabrication settings. We show how to accurately characterize anisotropy in these properties and when such characterization can be performed noninvasively. Our approach, when applied to 3D-printed stainless steel samples, reveals a significant heterogeneity between the surface and internal properties of the AM part and the anisotropy in material properties in the build and transverse directions.**

***Index Terms*—Pulse-echo ultrasound; Nanoindentation; Laser powder bed fusion; Anisotropy and material heterogeneity.**

I. Introduction

The question of whether additively manufactured (AM) components have the same material properties as traditionally manufactured parts is complex. The AM process parameters are known to influence such properties as density [1]–[3], strength [3]–[5], elasticity [6], microstructure [2]–[6], porosity [3], [5], and residual stresses [6], [7]. Therefore, the increased degrees of fabrication freedom that additive manufacturing introduces highlights the importance of better understanding the influence of the selected processing conditions on the material properties of the manufactured components.

Ultrasonic testing is primarily used in detecting fabrication defects and inclusions in metallic AM parts but rarely as a primary method for quantifying their material properties, with only a few studies using ultrasound to evaluate the elasticity, porosity, and density. For example, a purposeful echogenic segmentation of AL30/31 aluminum samples with small defects to localize the spatial variability in material properties suggested material homogeneity [8]. Homogeneity of aluminum samples was also reported in [9], [10]; a similar conclusion for titanium alloy AM parts was reached in [35]. However, anisotropy in AM aluminum alloy components was reported in [9], [10]. The anisotropy in 316L stainless steel AM parts was reported in [11].

This work was funded in part by the U.S. Department of Energy, National Energy Technology Laboratory, Award DE-FE0031559.

In this paper, we describe the use of ultrasonic measurements to reveal the material orthotropy and heterogeneity in stainless steel parts fabricated by the powder bed fusion (PBF), quantify the Poisson's ratio (ν), elastic and shear moduli (E and G), and the influence of PBF processing parameters on the material properties. The ultrasonically quantified properties are the aggregate values averaged along the length of the ultrasound preparation. We compared the material properties obtained from the ultrasonic data with local measurements obtained by the nanoindentation method [12] and found significant differences indicating material heterogeneity in the test samples.

II. Additive Manufacturing of test components

Three test samples with the dimensions (in mm) shown in Fig. 1a were 3D printed by PBF of a stainless-steel powder (EOS 316L powder, EOS GmbH, Krailling, Germany) using a direct metal laser sintering (DMLS) system with a 400 W peak-power laser beam (EOS M 280). The power density, E_d, of the scanning laser was varied in different segments of Parts Part V– and V+ (Fig. 1b) but was maintained constant at 33 $\mathrm{J/mm^3}$ in Part C.

III. Ultrasonic Characterization of Test Samples

The longitudinal and shear velocities were measured in pulse-echo mode using transducers with a 5 MHz central frequency exited by a square wave electrical pulse. Transducers were coupled to the test samples, as illustrated in the sidebar of Fig. 2a) and b), for measurements in build and transverse directions. The response was recorded with a 625 MHz sampling rate. The time of flight (TOF, t_{of}) through samples was measured as a delay between round-trip echoes, as illustrated in Fig. 2.

Table 1 shows the results for c_L and c_s in the build direction. The corresponding values of the Poisson's ratio, ν, and Young's and shear moduli, E and G, were calculated as follows, assuming material homogeneity, an assumption that is

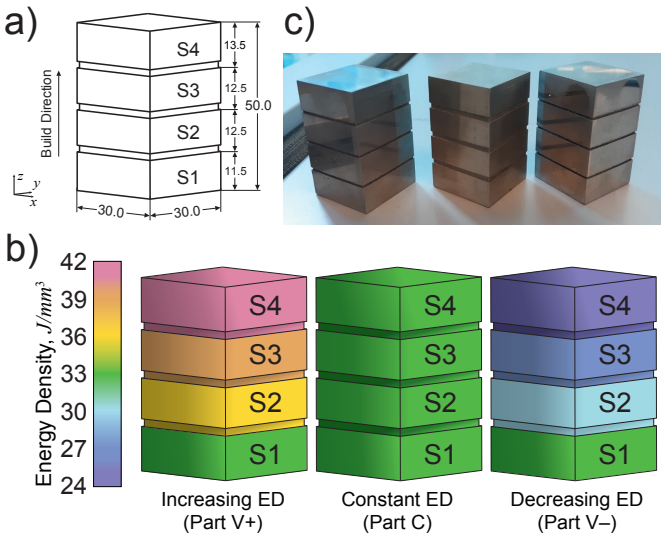

Fig. 1. a) Dimensions of test samples. b) Parts V+, C, and V– were produced with increasing, constant, and decreasing E_d, the values of which are color-coded. c) 3D printed 316L stainless steel parts.

TABLE I
ULTRASONIC VELOCITY AND AGGREGATE MATERIAL PROPERTIES IN THE BUILD DIRECTION.

Part	c_L [m/s]	c_s [m/s]	ν	E [GPa]	G [GPa]
V+	5160.92	2960.14	0.255	168.03	66.95
C	4718.10	2782.26	0.233	140.65	57.03
V–	4487.19	2654.21	0.231	125.18	50.80

violated in Parts V+ and V−, fabricated with changing energy density of the powder-melting laser:

$$\nu = \frac{1 - 2\left(\frac{c_s}{c_L}\right)^2}{2 - 2\left(\frac{c_s}{c_L}\right)^2} \tag{1}$$

$$c_L = \sqrt{\frac{E(1-\nu)}{\rho(1+\nu)(1-2\nu)}} \tag{2}$$

$$c_s = \sqrt{\frac{G}{\rho}} \tag{3}$$

The density, ρ, in these equations was obtained by weighing each part to 100 mg accuracy, determining its volume by dimensional measurements using a digital caliper to 10 μm accuracy, and adjusting the aggregate result to obtain segmental densities as a function of the laser's power and speed of scanning following the results reported by Kamath et al. [7].

Transverse ultrasonic data were acquired by coupling transducers to the sides of the segments, as illustrated in Fig. 2b (side panel), which shows typical pulse-echo waveforms for segment S1 of part V+ with marked first and second round-trip echoes, which we used to calculate transverse c_L and c_s.

Transverse ultrasonic data for different segments 3D printed with changing E_d was used in equations (1)–(3) to quantify the influence of the PBF parameters on the material properties of

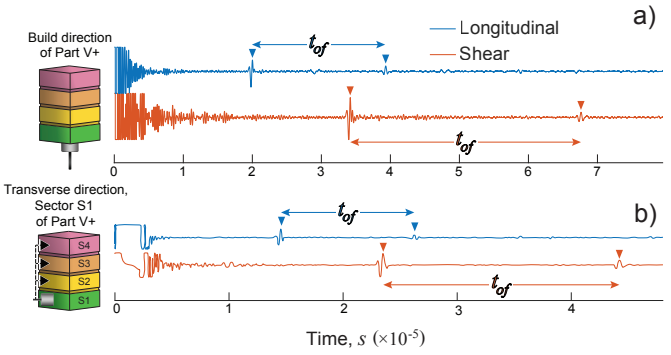

Fig. 2. a) Typical ultrasonic response in the build directions for part V+ (increasing E_d). The transducer was coupled to the bottom of segment S1 (side panel). Echoes, marked with color-coded triangles, reflected from the distal surface (the top of the S4 segment) correspond to one or more round trips through the sample. The delays between the second and first round trips, quantified by peak-to-peak tracking, were used to determine t_{of} for calculating c_L and c_s. b) Transverse ultrasonic responses for Part V+. Note the location of the transducer coupling in the side panel.

the fabricated stainless steel samples. Transverse longitudinal and shear wave velocities increased with increasing energy density (Fig. **??**a). Poisson's ratio ranged between 0.24 and 0.30 and increased with the energy density but decreased with the ratio c_s/c_L (results not shown), as would be expected from equation (1). Fig. **??**c shows the increase in Young's modulus with the energy density, which, according to equation (2), is attributable to the positive correlation of the longitudinal ultrasonic velocity and density with E_d. The increase in the shear modulus with the energy density, seen in Fig. **??**d, is expected from equation(3), which shows that G is increasing with both the shear wave velocity and the part's density. The difference between the transverse results in Fig. **??** with the corresponding results in the build direction, listed in Table I, especially revealing for the constant-energy-density Part C, indicates anisotropy in the material properties created by the layering process of additively manufacturing the stainless steel samples by PBF.

IV. NANOINDENTATION MEASUREMENTS

Polished test samples were placed on the nanoindenter stage (Hysitron TI Premier, Bruker Corp., Billerica, MA) and non-elastically deformed using a diamond tip, as confirmed by residual deformation seen in the SEM image in Fig. 4 (inset) after withdrawing the tip. Four force-displacement measurements, localized 2 nm apart in a square-like pattern, were averaged for each chosen location. The data were used to calculate the localized surface modulus and hardness of the test samples. We then profiled changes in these properties with the distance from the original test surface by removing thin layers of the material and repeating the nanoindentation measurements.

The comparison the surface values of Young's modulus measured by nanoindentation with the aggregate values (averaged transversely) measured ultrasonically shown in Fig. 4 reveals a large difference in the two values. Tested if the

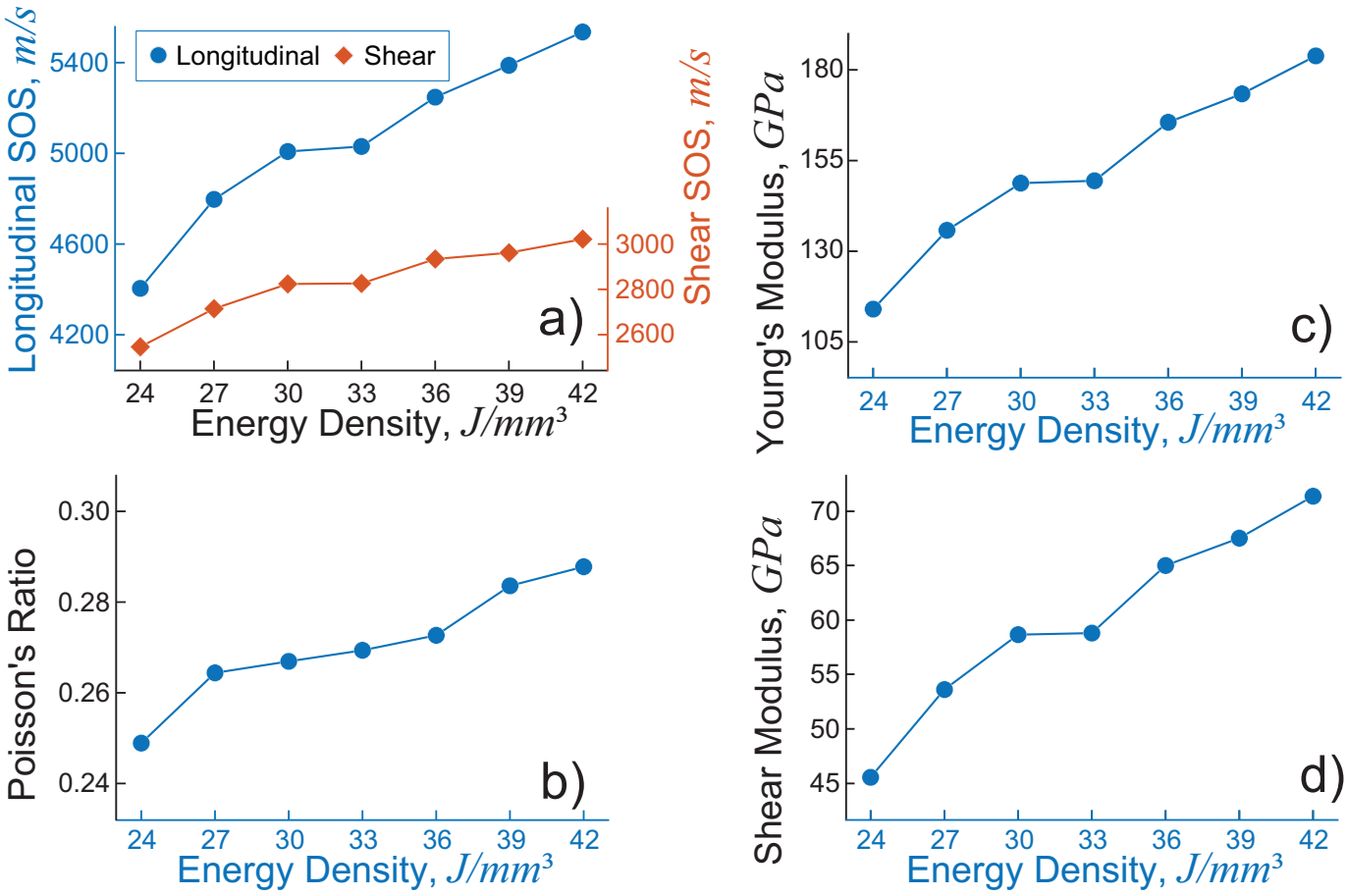

Fig. 3. a) Longitudinal and shear wave velocities increase with the energy density. Poisson's ratio b), Young's modulus c), and the shear modulus increased approximately linearly with increasing energy density.

observed difference could be attributed to changes in the material properties with distance from the surface by removing thin surface layers in the yz-plane of a sample and repeating nanoindentation and ultrasonic measurements. Fig. 5 shows that the two orthogonal type of measurements are converging as we move deeper into the sample. Specifically, while the ultrasonic measurements did not change significantly, the nanoindentation characterization shows significant decrease in Young's modulus from 207.02 GPa at the original surface to 178.38 GPa at the depth of 5.02 mm.

V. Conclusions

The ultrasonic characterization of 3D-printed metal components is highly sensitive to the material properties, including the anisotropy caused by the layering process and the effects of manufacturing conditions during the printing process on elastic moduli and Poisson's ratio. The pulsed-echo technique used by us and the pitch-catch characterizations aggregate the material properties along the length of the ultrasound propagation. When the ultrasound travels long distances through the material, its propagation velocity obtained from the pulse-echo data is an aggregate value insensitive to the localized variation in material properties. The comparison of the material properties obtained from such lumped results with the localized measurements obtained by nanoindentation revealed significant differences between the surface and interior properties of PBF-fabricated parts. This shows that the properties of parts fabricated by powder bed fusion can vary depending on the location, which is important to consider when choosing manufacturing conditions and post-fabrication treatments for these components.

Equations (1)–(3), used to estimate material properties from the ultrasonic data, assume isotropy of the propagation media. The comparison of the build and transverse direction measurements (Table I and Fig. 3) indicates material anisotropy. We addressed this inconsistency in a more detailed investigation [13], where we developed an approach based on the wave propagation model and the generalized Hook's law as the constitutive material model applicable in a more general case of anisotropic materials. We have shown in that study that in a particular case of weak anisotropy in build and transverse directions and transverse isotropy – conditions satisfied by the stainless steel test samples used in the current study – the errors introduced by applying equations (1)–(3) are small, as

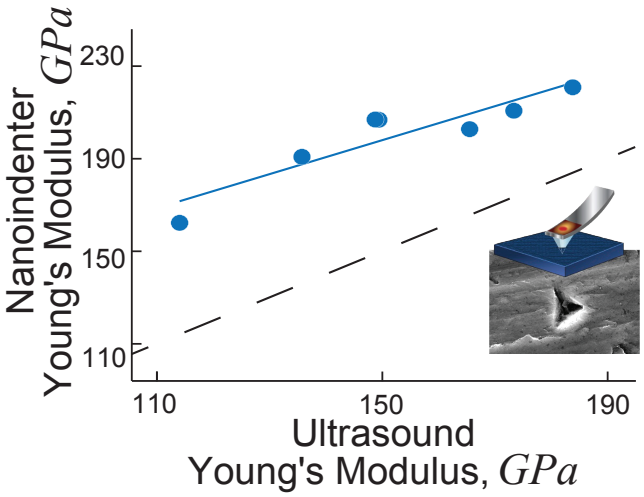

Fig. 4. Surface values of Young's modulus measured by nanoindentation exceeds the values measured ultrasonically that are not local and depend on values of E across the sample.

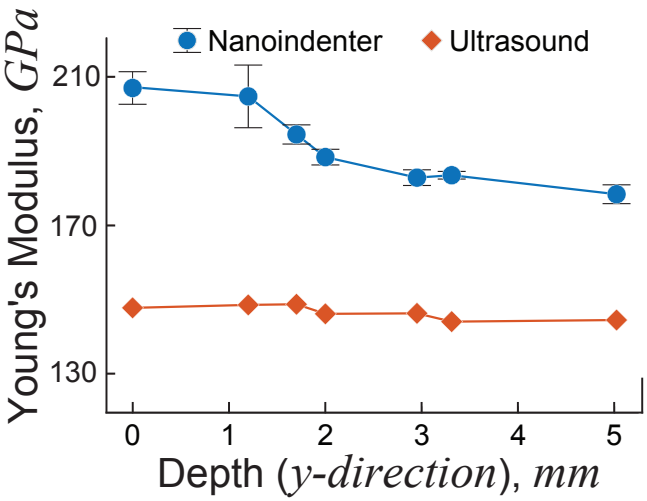

Fig. 5. Young's modulus measured by nanoindentation converges to the ultrasonic values with depth into the sample. The remaining difference is attributable to the bias in nanoindentation measurements (data not included)

long as the directions of the probing ultrasound are collinear and orthogonal to the build direction. Otherwise, additional ultrasonic measurements along the paths at carefully selected oblique angles to the build direction are necessary to estimate anisotropic material properties accurately.

ACKNOWLEDGMENT

This work was funded in part by the Department of Energy, National Energy Technology Laboratory (Award DE-FE0031559), an agency of the United States Government. The U.S. Government, any agency thereof, or any of its employees, makes any warranty, expressed or implied, or assumes any legal liability or responsibility for the accuracy, completeness, or usefulness of any information, apparatus, product, or process disclosed or that its use would not infringe privately owned rights. References herein to any specific commercial product, process, or service by trade name, trademark, manufacturer, or otherwise, do not necessarily constitute or imply its endorsement, recommendation, or favoring by the U.S. Government or any agency thereof. The views and opinions of the authors expressed herein do not necessarily state or reflect those of the U.S. Government or any agency thereof.

REFERENCES

[1] C. Kamath, B. El-Dasher, G.F. Gallegos, W.E. King, A. Sisto, "Density of additively-manufactured, 316L SS parts using laser powder-bed fusion at powers up to 400 W," Int J Adv Manuf Tech, vol. 74, pp. 65–78, 2014.

[2] S. Greco, K. Gutzeit, H. Hotz, B. Kirsch, J.C. Aurich, "Selective laser melting (SLM) of AISI 316L—impact of laser power, layer thickness, and hatch spacing on roughness, density, and microhardness at constant input energy density," Int J Adv Manuf Tech, vol. 108, pp. 1551–1562, 2020.

[3] N. Ahmed, I. Barsoum, G. Haidemenopoulos, R.K.A. Al-Rub, "Process parameter selection and optimization of laser powder bed fusion for 316L stainless steel: A review," J Manuf Process, vol. 75, pp. 415–434, 2022.

[4] A. Röttger, J. Boes, W. Theisen, M. Thiele, C. Esen, A. Edelmann, R. Hellmann, "Microstructure and mechanical properties of 316L austenitic stainless steel processed by different SLM devices," Int J Adv Manuf Tech, vol. 108, pp. 769–783, 2020.

[5] J. Liu, Y. Song, C. Chen, X. Wang, H. Li, C. Zhou, J. Wang, K. Guo, J. Sun, "Effect of scanning speed on the microstructure and mechanical behavior of 316L stainless steel fabricated by selective laser melting," Mater Des 186, 108355, 2020.

[6] B. Zhang, L. Dembinski, C. Coddet, "The study of the laser parameters and environment variables effect on mechanical properties of high compact parts elaborated by selective laser melting 316L powder," Mater Sci Eng A, vol. 584, pp. 21–31, 2013.

[7] A.J. Godfrey, J. Simpson, D. Leonard, K. Sisco, R.R. Dehoff, S.S. Babu, "Heterogeneity and solidification pathways in additively manufactured 316L stainless steels," Metall Mater Trans A, vol. 53, pp. 3321–3340, 2022.

[8] M. Roy, K. Walton, J.B. Harley, M. Skliar, "Ultrasonic evaluation of segmental variability in additively manufactured metal components," in IEEE Int Ultrason Symp (IUS), Kobe, Japan, https://doi.org/10.1109/ULTSYM.2018.8579663, 2018.

[9] T. Sol, S. Hayun, D. Noiman, E. Tiferet, O. Yeheskel, O. Tevet, "Non-destructive ultrasonic evaluation of additively manufactured AlSi10Mg samples," Addit Manuf, vol. 22, pp. 700–707, 2018.

[10] L. Hitzler, C. Janousch, J. Schanz, M. Merkel, F. Mack, A. Öchsner, "Non-destructive evaluation of AlSi10Mg prismatic samples generated by selective laser melting: influence of manufacturing conditions," in: Materwiss Werksttech, Wiley-VCH Verlag, pp. 564–581, 2016.

[11] K. Walton, M. Skliar, "Ultrasonic characterization of spatially varying material properties in metal components fabricated by additive manufacturing," in: IEEE Int Ultrason Symp (IUS), Glasgow, UK, 1260–1263, https://doi.org/10.1109/ULTSYM.2019.8925559, 2019.

[12] W.C. Oliver, G.M. Pharr, "An improved technique for determining hardness and elastic modulus using load and displacement sensing indentation experiments," J Mater Res, vol. 7, pp. 1564–1583, 1992.

[13] K. Walton, M. Skliar, "Ultrasonic Characterization of Material Heterogeneities in Stainless Steel Parts Fabricated by Powder Bed Fusion," unpublished.